Fe-Mg interdiffusion in wadsleyite: the role of pressure, temperature, composition and the magnitude of jump in diffusion rates at the 410 Km discontinuity

C. Holzapfel, S. Chakraborty, D.C. Rubie, D.J. Frost

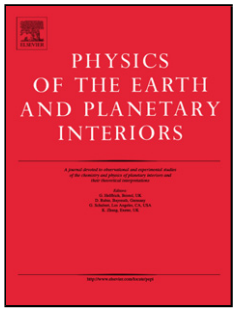

Title: Fe-Mg interdiffusion in wadsleyite: the role of pressure, temperature, composition and the magnitude of jump in diffusion rates at the 410 Km discontinuity

Authors: C. Holzapfel, S. Chakraborty, D.C. Rubie, D.J. Frost

PII: S0031-9201(08)00243-4
DOI: doi:10.1016/j.pepi.2008.09.005
Reference: PEPI 5062

To appear in: *Physics of the Earth and Planetary Interiors*

Received date: 4-12-2007
Revised date: 4-9-2008
Accepted date: 8-9-2008

Please cite this article as: Holzapfel, C., Chakraborty, S., Rubie, D.C., Frost, D.J., Fe-Mg interdiffusion in wadsleyite: the role of pressure, temperature, composition and the magnitude of jump in diffusion rates at the 410 Km discontinuity, *Physics of the Earth and Planetary Interiors* (2008), doi:10.1016/j.pepi.2008.09.005

Fe-Mg interdiffusion in wadsleyite: the role of pressure, temperature and composition and the magnitude of jump in diffusion rates at the 410 Km discontinuity

C. Holzapfel[1*], S. Chakraborty[2**], D.C. Rubie[1], D.J. Frost[1]

[1]Bayerisches Geoinstitut, Universität Bayreuth, D-95440 Bayreuth, Germany

[2]Institut für Geologie, Mineralogie und Geophysik, Ruhr Universität Bochum, D-44780 Bochum, Germany.

[*]Now at:

Schleifring und Apparatebau GmbH,
Am Hardtanger 10,
D-82256 Fürstenfeldbruck,
Germany,

email: cholzapfel@schleifring.de

** Corresponding Author

email: Sumit.Chakraborty@rub.de

Abstract

The limited stability range of wadsleyite seriously impedes our ability to constrain kinetic parameters (e.g. activation energy, activation volume) using experiments carried out over a wide range of temperature and pressure. We have carried out a new measurement to extend the experimental temperature range of the dataset of Chakraborty et al. (1999) to the maximum possible limit for that experimental setup. This result allows us to (i) obtain a better constrained value for activation energy for Fe-Mg diffusion in wadsleyite at 15 GPa (~ 230 kJ/mol), and (ii) characterize the compositional dependence of Fe-Mg diffusion in wadsleyite. Evaluation of all data available in the literature (i.e. this study, Chakraborty et al., 1999; Farber et al., 2000 and Kubo et al., 2004) reveals that there is a strong pressure dependence of the diffusion coefficient (activation volume ≈ 14 cm^3/mol). The expression

$$D(\mathrm{m^2/s}) = 1.24 \cdot 10^{-6} . \exp\left[11.8\left(0.86 - X_{\mathrm{Mg}}\right)\right] \cdot \exp\left(\frac{-\left[229000 + (P-15)\cdot 13.9 \cdot 10^3\right]\mathrm{J/mol}}{RT}\right)$$

is an excellent description of all experimentally measured diffusion coefficients in wadsleyite and points to consistency between the various studies from different laboratories that used different methods. This expression should provide a robust basis for extrapolation of diffusion data for wadsleyite to conditions removed from the experimental ones, e.g. for modeling processes in the interiors of cold subducting slabs. Moreover, characterization of fO_2 and water contents of wadsleyites in the current study and consideration of the pressure dependence of diffusion rates in olivines confirms that the jump in diffusion rates at the olivine - wadsleyite boundary in the transition zone is at least 6 orders of magnitude; increased water contents in wadsleyite can cause the actual enhancement (Kubo et al., 2004) to be as much as 7 orders of magnitude. Taken together with the observation that diffusive mixing is practically impossible in the lower mantle (Holzapfel et al., 2005), has a maximum at the lithosphere - asthenosphere boundary in the olivine-bearing upper mantle (Holzapfel et al., 2007), and decreases with depth within the transition zone (this work), these results establish the base of the lithosphere and the top of the mantle transition zone as the key regions for mixing and erasure of chemical heterogeneities in the mantle.

Keywords: Diffusion, Pressure, Activation volume, Activation energy, Wadsleyite, Olivine, Multianvil, Mantle transition zone, Olivine-wadsleyite phase transition.

1. Introduction

Knowledge of diffusion rates of atoms in minerals of the mantle transition zone is important for understanding rates of chemical equilibration and mixing in this region as well as for the modeling of physical processes such as creep and electrical conductivity. In spite of their importance, diffusion coefficients are particularly difficult to determine because of (a) the difficulty in obtaining suitable material for diffusion experiments, (b) the usual uncertainties of obtaining diffusion data from high pressure experiments, i.e. the precise control of ambient variables such as temperature, pressure and oxygen fugacity is difficult, and (c) the narrow stability range of some of the high pressure phases at temperatures where diffusion experiments can be carried out. This last aspect precludes obtaining Arrhenius equation parameters (activation energies and volumes) from experiments carried out over a wide range of pressures and temperatures, even if difficulties (a) and (b) were to be overcome through innovative experimental strategies. The situation is aggravated by the fact that the few available data on diffusion rates in wadsleyite (Chakraborty et al., 1999; Farber et al., 2000 and Kubo et al., 2004) appear to be inconsistent with each other or, in an alternative interpretation, are scattered over a wide range. This aspect becomes critical when one needs to extrapolate these data to lower temperatures to calculate, for example, the kinetics of conversion of olivine to wadsleyite in the interior of relatively-cold subducting slabs.

To address this issue, we have carried out an additional, key experiment and analysed the available data to exploit subtle systematics in the "scatter" noted above in order to retrieve an activation energy and activation volume that reproduces all available data surprisingly well. Additionally, the activation energy that is obtained is consistent with that obtained for Fe-Mg diffusion in other spinel structures (Liermann and Ganguly, 2002; Sheng and Wasserburg, 1992), giving confidence that our results may be used for the reliable extrapolation of diffusion data.

2. Previous Work

Only three studies exist in which Fe-Mg interdiffusion coefficients for wadsleyite were measured. All studies [Chakraborty et al., 1999; Farber et al., 2000 and Kubo et al., 2004] showed a marked increase in diffusivity of 2-3 orders of magnitude across the olivine-wadsleyite phase boundary. In the study of Chakraborty et al. (1999), only two experiments, at 1373 and 1473 K, were performed on wadsleyite, and these results are subject to uncertainties in oxygen fugacity that have been discussed in detail in Holzapfel et al. (2007). Consequently, we have measured an additional data point at a different temperature and used the improved characterization of the ambient oxygen fugacity conditions (Holzapfel et al., 2007) to better constrain the activation energy of diffusion in wadsleyite. We use this result in conjunction with data from Farber et al. (2000) and Kubo et al. (2004) to constrain the activation volume of diffusion.

3. Experimental

3.1. Starting material

Wadsleyite diffusion couple experiments, employing a single crystal as one endmember, are described by Chakraborty et al., (1999), but we failed to synthesize large enough crystals for this study. Therefore, polycrystalline wadsleyite samples were synthesized prior to diffusion runs as starting material. For all synthesis experiments a 14/8 multianvil sample assembly (see below and Holzapfel et al., 2007 for a detailed description) and Re capsules were used. A polycrystalline pure Mg_2SiO_4 wadsleyite sample was prepared by annealing forsterite powder at 15 GPa and 1673 K in a 1000 t multianvil press. For the Fe-bearing sample, a single crystal of olivine from San Carlos, with Fe/(Fe+Mg) = 0.16, kindly provided by S. Mackwell, was annealed at 15 GPa and 1873 K. Another Fe-bearing wadsleyite sample was synthesized from hot-pressed San Carlos olivine powder at 15 GPa and 1673 K in a Re-capsule. Raman spectroscopy using a LabRAM microraman instrument (Jobin Yvon GmbH) and X-ray microdiffraction showed the synthesized material to be wadsleyite in all cases.

After synthesis the samples were removed from the high-pressure assembly and the

Re foil capsule was peeled off. Subsequently the cylindrical wadsleyite samples were cut into discs ~ 250 μm thick and mounted on glass slides in order to polish them using diamond compounds. After polishing, small discs were drilled out for use in diffusion couples.

3.2. Capsule Material

The diffusion anneal at high pressure was carried out in a Ni capsule produced from Ni foil (thickness 125 μm, 99.98% Goodfellow). The two polycrystalline slices of wadsleyite were placed with their polished faces in contact, and the material was covered by NiO powder that was previously dried at 1273 K. This setup constrains the oxygen fugacity to lie at the NNO buffer and close to that obtained intrinsically in a Au capsule (Holzapfel et al. 2007), and the silica activity is constrained by the equilibrium $2Ni + SiO_2 = Ni_2SiO_4$.

3.3. High-Pressure Diffusion Anneal

The high-pressure diffusion anneal was carried out at 15 GPa and 1773 K for 16 minutes using a 1000 t split-cylinder multianvil apparatus. The pressure assembly consisted of a MgO octahedron with 14 mm edge length as the pressure medium and WC cubes with a truncation edge length of 8 mm (14/8 assembly), which is identical to the one illustrated in Holzapfel et al. (2007). Heating was performed with a stepped $LaCrO_3$ resistance furnace, thus ensuring that temperature gradients do not exceed 20 K mm^{-1} (Rubie et al., 1993). Pressure was calibrated using the quartz-coesite and Mg_2SiO_4 olivine-wadsleyite transformations (Keppler and Frost, 2005). After heating to 1773 K, the temperature was controlled to within ±1 K. The sample was quenched by switching off the power to the furnace, which resulted in the temperature dropping to below 573 K in less than 2 sec. This run condition is at a higher temperature, but at the same pressure and at a defined oxygen fugacity that is similar to that of the experiments of Chakraborty et al. (1999), and can thus be used to better constrain the temperature dependence of the diffusion coefficient. Simple numerical simulations indicate that for realistic values of activation energies and diffusion coefficients, it is not necessary to correct for diffusion that occurred during the heat up time (at 2 K / sec). In experiments that we performed at lower temperatures (e.g. 1673 K)

ringwoodite began to form in the compositions of our choice and results from these experiments are therefore not considered further for obtaining diffusion coefficients.

4. Profile analysis and diffusion coefficient determination

After the experiment, the octahedron was mounted in epoxy resin and ground and polished until the middle of the diffusion couple was exposed (Fig. 1). Concentration profiles were measured using an electron microprobe (Cameca SX-50 equipped with 4 wavelength dispersive spectrometers and operating at 15 kV, 15nA). Special attention was paid to optimize the lateral spatial resolution of the microprobe beam by aligning the objective aperture with the help of a cathodoluminenscence spot on SnO_2 and by correcting for astigmatism at high magnifications. San Carlos olivine was used as the standard for quantification of all major elements. Strongly asymmetric diffusion profiles were observed which could be modelled by finite difference simulation using a exponential composition dependence. The algorithm is the same as that used by Holzapfel et al. (2003) for simulation of asymmetric profiles in ferropericlase diffusion couples.

5. Results

5.1. Backscatter images and sample characterization

Backscatter and orientation contrast imaging reveals that grain sizes on the Fe-rich side of the diffusion couple are on the order of 25 μm. On the Mg-rich side, grains of approximately 60 μm are found which show a pervasive deformation microstructure. The large grains are recrystallized into subgrains of ~ 1 μm during the high-pressure, high-temperature anneal. Potentially this could lead to enhanced diffusion like that found in the feldspar system by Yund and Tullis (1991). However, careful observation of the diffusion zone by backscatter imaging and elemental mapping does not reveal any significant disturbance of the diffusion front, as would be expected if grain boundary diffusion had played an important role. We note here that grain boundary diffusion is likely to dominate at lower temperatures and therefore the observation of no grain boundary enhancement of diffusion rates at the high temperature of this experiment is entirely consistent with expectations from diffusion theory (e.g. see

Manning, 1974; Chakraborty, 2008).

On the Fe-free side of the interface, the backscatter image of the sample, together with element mapping, reveals the presence of a silica-rich phase with enstatite stoichiometry, in addition to wadsleyite. This phase is interpreted to result from the synthesis where the stoichiometry of the starting mixture must not have been in the exact proportions. If the presence of enstatite had resulted from Fe uptake by the Ni capsule, the enstatite inclusions would be confined to or at least concentrated near the outer rim of the diffusion couple, which is not the case. Furthermore, measurements in the Ni capsule did not reveal any increase in Fe at the contact with the sample.

Because wadsleyite can potentially accommodate several thousand ppm of water (Smyth, 1987, McMillan et al., 1991, Kohlstedt et al., 1996), IR-spectroscopy was performed which indicated water concentrations of around 35 ppm (Fig. 2) for both endmembers (Paterson, 1982). This is an extremely low water content for wadsleyite, indicating that the results presented here are representative of essentially-dry wadsleyite. The study of Kubo et al., 2004 showed that there is a strong influence of water on Fe-Mg interdiffusion in wadsleyite. Hier-Majumder et al. (2004), Demouchy et al. (2007), Costa and Chakraborty (2008) and Wang et al. (2004) have demonstrated that water enhances diffusion rates in other mantle phases.

5.2. Profiles

Figure 3a shows representative Fe and Mg concentration profiles. Both profiles show a marked asymmetry, implying that the Fe-Mg interdiffusion coefficient is strongly composition-dependent. A numerical simulation was carried out, as noted above, to retrieve compositionally-dependent diffusion coefficients given by $D^{Wds}_{Fe\text{-}Mg}(X_{Fe}) = D^{Wds}_{Fe\text{-}Mg}(X_{Fe} = 0) \exp(11.8\, X_{Fe2SiO4})$. At the run conditions of this experiment (run # C45, 15 GPa, 1773 K, f_{O2} = NNO, 16 min.), $D^{Wds}_{Fe\text{-}Mg}(X_{Fe} = 0) = 4.7 \times 10^{-14}$ m^2/s. Calculated concentration profiles using the retrieved diffusion coefficients are also shown in Fig. 3a for comparison and it is seen that an exponential composition dependence, qualitatively analogous to that found in olivine (Chakraborty, 1997; Dohmen et al., 2007), also reproduces the observed asymmetry of the profiles in wadsleyite.

The relatively strong asymmetry of the profiles shown in Fig. 3a contrasts with the symmetry of the profile shown for wadsleyite interdiffusion experiments in Fig. 3a of Chakraborty et al. (1999). This difference arises because the range of compositions used in the latter study was small (X_{Fe} ranged from 0.10 to 0.18). Figure 3b shows that the data from run # H654 of Chakraborty et al. (1999) (15 GPa, 1200 °C, 24 hours) can be described just as well using the same compositional dependence as that obtained above and that over this narrow compositional range the calculated profile is indeed symmetric.

5.3. Composition and temperature dependence at 15 GPa

As noted by Chakraborty et al. (1999), their estimated activation energy for Fe-Mg interdiffusion was of a very preliminary nature because it was based on only two data points that were obtained over a restricted temperature range (1100 and 1200 °C). The addition of the new result from this study, obtained at 1500 °C at the same pressure (15 GPa) and oxygen fugacity (close to NNO buffer, see Holzapfel et al., 2007) and the same experimental protocoll considerably improves the situation. When diffusion coefficients calculated at a constant median composition of X_{Fe} = 0.14 using the above compositional-dependence are plotted on an Arrhenius diagram (Fig. 4a), data points from the three experiments lie on a well defined isobaric Arrhenius line given by 1.24×10^{-6} exp (-229 kJ/mol/RT) m^2/sec. Here, 229 kJ/mol refers to the activation energy for Fe-Mg diffusion at 15 GPa and is considerably larger than the preliminary value of 145 kJ/mol given by Chakraborty et al. (1999). If a formal fitting is carried out, the nominal statistical errors yield and uncertainty of ± 27 kJ/mol for the activation energy.

5.4. Comparison with previous studies and the effects of pressure and water content

Kubo et al. (2004) and Farber et al. (2000) have also determined Fe-Mg diffusion rates in wadsleyite using diffusion couples with different mean compositions and from experiments carried out at different pressures; in the case of Kubo et al. (2004),

measurements were also made on wadsleyites with different water contents. All of the experiments were carried out at oxygen fugacities close to that of the NNO buffer at the respective P-T conditions. When all diffusion coefficients obtained under nominally dry conditions are normalized to the same composition (X_{Fe} = 0.14) using the relationship obtained above, it appears, on first sight, that there is a large scatter (Table 1, Fig. 4b). However, on closer inspection it is found that data obtained from higher pressure experiments yield systematically smaller diffusion coefficients, suggesting that the scatter may result from the effect of pressure on diffusion. Consequently, we tested the following hypothesis: If a pressure dependence is determined using data from our laboratory obtained at 15 GPa (Fig. 4a) and that from any one other pressure, does the resulting pressure dependence allow all other diffusion coefficients in the literature (Fig. 4b) to be adequately described? Using any one of the other data points in combination with our data, we consistently obtain an activation volume of about 13 × 10^{-6} m^3/mol for Fe-Mg diffusion in wadsleyite. Therefore, we decided to take all of the remaining data from the literature (i.e. Kubo et al., 2004 and Farber et al., 2000) in combination with the composition and temperature dependences obtained above to constrain the pressure dependence of Fe-Mg diffusion in wadsleyite. The resulting activation volume of 13.9 (±1.5) × 10^{-6} m^3/mol is found to describe all available diffusion data in Fe-Mg wadsleyite rather well (Fig. 4c).

Combining these results, we can obtain the following global relationship for Fe-Mg diffusion in wadsleyite under dry conditions and with fO_2 lying along the NNO equilibrium:

$$D(\mathrm{m^2/s}) = 1.24\cdot 10^{-6}\cdot \exp\left[11.8\left(0.86 - X_{\mathrm{Mg}}\right)\right]\cdot \exp\left(\frac{-\left[229000 + (P-15)\cdot 13.9\cdot 10^3\right]\mathrm{J/mol}}{RT}\right)$$

where “dry conditions” means up to several 10's of ppm H_2O (Kubo et al., 2004). Here, P is in gigapascals, T is absolute temperature and X_{Mg} is the mole fraction of the Mg-endmember. Fig. 4c shows that this relationship is an excellent description of all data from all three laboratories. If the effect of water on diffusion observed by Kubo et al., 2004 at 1230 °C is independent of temperature and water content, then diffusion in wet wadsleyite (several 100 ppm or more of H_2O) would be an order of magnitude

faster than that calculated using the above relation. To determine diffusion coefficients in wadsleyite at other oxygen fugacities, it is necessary to know the fO_2 dependence of diffusion, which is currently not known. Therefore, the relationship should be restricted to the calculation of diffusion coefficients at oxygen fugacities at or near the NNO buffer. At more reducing conditions, the calculated diffusion coefficients are likely to be overestimates. In the absence of other constraints, an approximate estimate of the magnitude of this effect may be obtained by using the f_{O2} dependence of Fe-Mg diffusion coefficients observed for olivine (e.g. see Holzapfel et al., 2007, Dohmen and Chakraborty, 2007).

7. Implications

In spite of indications that diffusion in wadsleyite is faster than in olivine at similar conditions by about three to four orders of magnitude (Chakraborty et al., 1999; Farber et al., 2000), there have been questions as to whether uncertainties in fO_2 and fH_2O have compromised this conclusion (e.g. Kubo et al., 2004). Now that relationships have been established to calculate Fe-Mg diffusion coefficients in nominally dry (up to a few 10's of ppm H_2O) olivine and wadsleyite (Holzapfel et al., 2007; Dohmen and Chakraborty, 2007; Chakraborty et al., 1999; Farber et al., 2000; Kubo et al., 2004; this work) as a function of P, T and composition, we can compare the diffusion rates in these two minerals at conditions where they coexist in equilibrium at the top of the transition zone (410 km seismic discontinuity). Using data from the experimental work of Katsura et al. (2004), we find that the transition occurs at 13 GPa, 1750 K and the compositions of coexisting olivine and wadsleyite are X_{Mg} = 0.91 and 0.86, respectively. The diffusion coefficients in olivine and wadsleyite at these P, T, X conditions are given by 1.3 x 10^{-18} m^2/ sec and 1.2 x 10^{-12} m^2/sec, respectively, if the fO_2 is at or close to that of the NNO buffer i.e. there is a jump in diffusion rates of 6 orders of magnitude at the transition. Conversely if olivine survives metastably in the interior of slabs, diffusive and mixing proccesses would be retarded by the same factor. This magnitude of jump in diffusivity is not changed if bulk compositional constraints for the mantle are used to compare diffusivities in olivine and wadsleyite at a composition of X_{Mg} ~ 0.9 for both, over a range of P-T conditions between 13 – 14 GPa and 1700 – 1750 K.

The jump in diffusion rates inferred above is a minimum estimate, because water partitions strongly between olivine and wadsleyite (Bolfan-Casanova et al., 2000). Due to this partitioning, olivine coexisting with wadsleyite is likely to be relatively dry (< 20 ppm H_2O) whereas wadsleyite may contain up to several hundred ppm H_2O. This would imply another order of magnitude increase in the diffusion coefficients in wadsleyite, leading to a total jump in diffusion rates at the top pf the transition zone of 7 orders of magnitude. The large change in diffusivity across this boundary reinforces the conclusion that reequilibration is much more efficient in the transition zone than in the upper mantle (see Chakraborty et al., 1999; Farber et al., 2000 and Kubo et al., 2004 for earlier inferences). However, the large activation volume of diffusion implies that diffusion rates in wadsleyite decrease rapidly and non-linearly with pressure, although these rates remain much faster than those in olivine at all conditions. If it is assumed that diffusion rates in ringwoodite are very similar to those in wadselyite, then the activation volume obtained in this work suggests that diffusion rates in the top 100 Km or so of the transition zone (at depths between 400 and 500 Km) are much faster than the rates at greater depths.

Holzapfel et al. (2004) have shown that extremely sluggish diffusion in perovskite practically precludes diffusive mixing in the lower mantle. On the other hand, Holzapfel et al. (2007) show that diffusion is most efficient at the lithosphere - asthenosphere boundary in the olivine-bearing part of the mantle. Combined with the results for wadsleyite, we can identify the top of the transition zone and the lithosphere - asthenosphere boundary as the two depths in the mantle where transport is most efficient, making these the primary sites for chemical homogenization and erasure of heterogeneities.

8. Conclusions

It has been shown that the activation energy for Fe-Mg diffusion in wadsleyite at 15 GPa (~ 229 kJ/mol) is similar to that for Fe-Mg diffusion rates in other spinels that are stable at atmospheric pressure (e.g. ~200 kJ/mol, Liermann and Ganguly, 2002) and the diffusion rate has a relatively strong pressure dependence described by an activation volume of ~14 x 10^{-6} m^3/mol. The diffusion rate in wadsleyite depends on

composition, with diffusion rates increasing with Fe-content in an exponential manner similar to that found for olivine: $D^{Wds}_{Fe\text{-}Mg}$ (X_{Fe}) = $D^{Wds}_{Fe\text{-}Mg}$ (X_{Fe} = 0) exp (11.8 $X_{Fe2SiO4}$). Combined with constraints on water contents and oxygen fugacities of the experimental diffusion anneals, it is now possible to calculate diffusion coefficients in wadsleyite as a function of pressure, temperature, composition and water content over a wide range of conditions, although uncertainty remains about the f_{O2} dependence of the diffusivities. Knowledge of diffusivity as a function of these variables in olivine (Dohmen and Chakraborty, 2007, Holzapfel et al., 2007) as well as wadsleyite (this work) now demonstrates convincingly that at the boundary between the upper mantle and the transition zone diffusivities jump by at least 6 and may be 7 orders of magnitude (depending on the exact content and distribution of water in the mantle). The activation volume of diffusion obtained in this work implies that diffusion rates decrease rapidly and non-linearly with depth within the transition zone. In combination with results from earlier diffusion studies (Holzapfel et al., 2005, Holzapfel et al., 2007), this allows us to identify the lithosphere - asthenosphere boundary and the top of the transition zone as the two key regions for chemical mixing in the mantle.

9. Acknowledgments

We thank the German Science Foundation (DFG) for supporting our research and Hubert Schulze in Bayreuth for sample preparation. Tomoaki Kubo and an anonymous reviewer are thanked for their constructive reviews.

10. References

Bolfan-Casanova, N., Keppler, H., and Rubie, D., 2000, Water partitioning between nominally anhydrous minerals in the MgO-SiO2-H2O system up to 24 GPa: Implications for the distribution of water in the Earth's mantle.: Earth Planet. Sci. Lett., 182: 209-221.

Chakraborty, S., 2008. Diffusion in solid silicates - a tool to track timescales of processes comes of age, Annual Reviews of Earth and Planetary Science, 36:153-190.

Chakraborty, S., 1997. Rates and mechanisms of Fe-Mg interdiffusion in olivine at 980-1300 °C. J. Geophys. Res., 102: 12317-12331.

Chakraborty, S., Knoche, R., Schulze, H., Rubie, D. C., Dobson, D., Ross, N.L., and Angel, R.J., 1999. Enhancement of cation diffusion rates across the 410-kilometer discontinuity in Earth's mantle. Science, 283: 362-365.

Costa, F., and Chakraborty, S., 2008, The effect of water on Si and O diffusion rates in olivine and implications for transport properties and processes in the upper mantle: Phys. Earth Planet. Inter., v. 166:11-29.

Demouchy, S., Mackwell, S.J., and Kohlstedt, D.L., 2007, Influence of hydrogen on Fe-Mg interdiffusion in (Mg,Fe)O and implications for Earth's lower mantle: Contrib. Mineral. Petrol., v. 154, p. 279-289.

Dohmen, R., Becker, H.-W, and Chakraborty, S. (2007) Fe-Mg diffusion coefficients in olivine. Part I: Experimental determination between 700 and 1200 °C as a function of composition, crystal orientation and oxygen fugacity. Physics and Chemistry of Minerals, Doi 10.1007/s00269-007-0157-7, 19 pages.

Dohmen, R. and Chakraborty, S. (2007) Fe-Mg diffusion in olivine II: Point defect chemistry, diffusion mechanisms and a model for calculation of diffusion coefficients in natural olivine. Physics and Chemistry of Minerals, Doi10.1007/s00269-007-0158-6, 22 pages.

Farber, D. L., Williams, Q., and Ryerson, F.J. 2000. Divalent cation diffusion in Mg_2SiO_4 spinel (ringwoodite), β - phase (wadsleyite), and olivine: Implications for the electrical conductivity of the mantle. J. of Geophy. Res., 105: 513-529.

Hier-Majumder, S., Anderson, I.M., and Kohlstedt, D.L., 2004, Influence of Protons on Fe-Mg interdiffusion in olivine: J. Geophys. Res., v. 110, p. doi: 10.1029/2004JB003292.

Holzapfel, C., Rubie, D. C., Mackwell, S., and Frost, D. J., 2003. Effect of pressure on Fe-Mg interdiffusion in (Fe,Mg)O, ferropericlase. Phys. Earth Planet. Int., 139: 21-34.

Holzapfel, C., Rubie, D. C., Frost, D. J., and Langenhorst, F., 2005, Fe-Mg interdiffusion in (Mg.Fe)SiO_3 perovskite and lower mantle reequilibration, Science, 309: 1707 - 1710.

Holzapfel, C., Chakraborty, S., Rubie, D.C. and Frost, D.J. (2007) Effect of pressure on Fe-Mg, Ni and Mn diffusion in $(Fe_xMg_{1-x})_2SiO_4$ olivine, Phys. Earth Planet. Int. 162: 186 - 198.

Katsura, T., Yamada, H., Osamu Nishikawa, O., Song, M., Kubo, A., Shinmei, T., Yokoshi, S., Aizawa, Y., Yoshino, T., Walter, M.J. and Ito, E. (2004) Olivine-wadsleyite transition in the system $(Mg, Fe)_2SiO_4$. J. Geophys. Res. 109, B02209, doi: 10.1029/2003JB002438.

Keppler, H. and Frost, D.J. (2005) Introduction to minerals under extreme conditions. In: Miletich, R. (Ed.), Mineral Behavior at Extreme Conditions, European

438 Mineralogical Union Lecture Notes in Mineralogy, vol. 7. EMU, pp. 1-30.
439
440 Kohlstedt, D. L., Keppler, H. and Rubie, D. C., 1996. Solubility of water in the α, β,
441 and γ phases of $(Mg,Fe)_2SiO_4$. Contrib. Mineral. Petrol., 123: 345-357.
442
443 Kubo, T., Shimojuko, A., and Ohtani, E. 2004 Fe-Mg interdiffusion rates in
444 wadsleyite and the diffusivity jump at the 410 km discontinuity. Phys. Chem.
445 Minerals, 31: 456-464
446
447 Liermann HP, Ganguly J. 2002. Diffusion kinetics of Fe2+ and Mg in aluminous
448 spinel: experimental determination and applications. Geochim. Cosmochim. Acta. 66:
449 2903–2913
450
451 Manning, D.R. (1974) Diffusion kinetics and mechanisms in simple crystals, In: A.
452 W. Hoffmann, B. J. Giletti, H. S. Yoder, and R. A. Yund (Editors) Geochemical
453 Transport and Kinetics. Carnegie Institution of Washington, –3-13.
454
455 McMillan, P.F., Akaogi, M., Sato, R.K., Poe, B. and Foley, J. (1991) Hydroxyl
456 groups in β-Mg_2SiO_4, Amer. Mineral., 76:354-360.
457
458 Paterson, M. S., 1982. The determination of hydroxyl by infrared absorption in quartz,
459 silicate glasses and similar materials. Bull. Mineral., 105: 20-29.
460
461 Rubie, D. C., Karato, S., Yan, H., and O'Neill, H. S. C., 1993. Low differential stress
462 and controlled chemical environment in multianvil high-pressure experiments. Phys.
463 Chem. Min., 20: 315-322.
464
465 Sheng, Y. J. and Wasserburg, G. J. (1992). Self- diffusion of magnesium in spinel and
466 in equilibrium melts: constraints on flash heating of silicates. Geochimica et
467 Cosmochimica Acta 56: 2535-2546.
468
469 Smyth, J.R. (1987) β-Mg_2SiO_4: A potential host for water in the mantle? Amer.
470 Mineral. 72:1051-1055.
471
472 Wang, Z., Hiraga, T., and Kohlstedt, D.L., 2004, Effect of H^+ on Fe-Mg interdiffusion
473 in olivine, $(Fe\text{-}Mg)_2SiO_4$: Appl. Phys. Lett., v. 85, p. 209-211.
474
475 Yund, R. A., Tullis, J., 1991. Compositional changes of minerals associated with
476 dynamic recrystallization. Contr. Min. Petrol., 108: 346-355.

Figure captions

Figure 1. Electron Backscatter image of sample C45 annealed at 1773 K, 15 GPa for 16 minutes in a 14/8 assembly. Concentration profiles were measured in the regions well removed from the cracked zone.

Figure 2. Unpolarized FTIR spectrum of $(Mg,Fe)_2SiO_4$ wadsleyite from experiment C45 synthesised at 15 GPa and 1773 K. The absorption coefficient is normalised to a thickness of 1 cm. The absorption bands are consistent with previous measurements (e.g. Kohlstedt et al. 1996) and attributed to OH defects in the crystal structure of wadsleyite. The H_2O content is estimated to be approximately 35 ppm, which is one order of magnitude lower than previous H_2O measurements on wadsleyite synthesised under nominally anhydrous conditions (McMillan et al. 1991).

Figure 3a. Representative Fe and Mg profiles (symbols) measured by electron microprobe on sample C45. The sample was annealed at 15 GPa, 1773 K for 16 minutes and the fit (line) is calculated according to the compositionally dependent expression given in the text.

Figure 3b. Comparison of a numerical profile simulation using values for the composition dependence obtained at high temperature in this study, as described in the text, and an Fe-Mg profile of sample H654 from the study of Chakraborty et al. (1999).

Figure 4a. Logarithm of the Fe-Mg interdiffusion coefficient for wadsleyite at 15 GPa as a function of inverse temperature obtained in this study (one datum) and by Chakraborty et al., 1999 (two data points). The datum of this study is for the composition $X_{Fe} = 0.14$, the average composition of the earlier study of Chakraborty et al., 1999. As described in the text, the activation energy is derived by fitting all data simultaneously.

Figure 4b. Logarithm of Fe-Mg interdiffusion coefficients for wadsleyite measured in different studies (this work, Chakraborty et al., 1999; Farber et al., 2000, Kubo et al., 2004). All experiments were carried out at oxygen fugacities close to that of the NNO buffer. The experimental anneals were carried out at different pressures.

Figure 4c. Lines showing variation of Fe-Mg diffusion in wadsleyite as a function of temperature at different pressures (from top down: 13 GPa, 15 GPa, 16 GPa and 17 GPa). The calculations are based on the retrieved activation volume of 13.9×10^{-6} m^3/mol. The symbols represent measured data points - square: Farber et al., 2000 at 13 GPa, solid circle: Chakraborty et al., 1999, open circles: Kubo et al., 2004 at 16, 16.5 and 17 GPa, and diamond: this study, 15 GPa.

Table 1: Summary of Fe-Mg diffusion data in wadsleyite from this and other studies in the literature (Chakraborty et al., 1999; Farber et al., 2000; Kubo et al., 2004), all normalized to a composition of X_{Fe} = 0.14 using the composition dependence found in this study.

Source	P(GPa)	T(K)	D (m^2/s)	Log_{10} D
This work	15	1673	3.43E-13	-12.47
Chakraborty'99	15	1473	7.00E-15	-14.16
Chakraborty'99	15	1373	3.00E-15	-14.52
Farber'00	13	1473	5.00E-14	-13.30
Kubo'04	16	1503	4.13E-15	-14.38
Kubo'04	16.5	1703	1.97E-14	-13.71
Kubo'04	17	1803	4.13E-14	-13.38

532

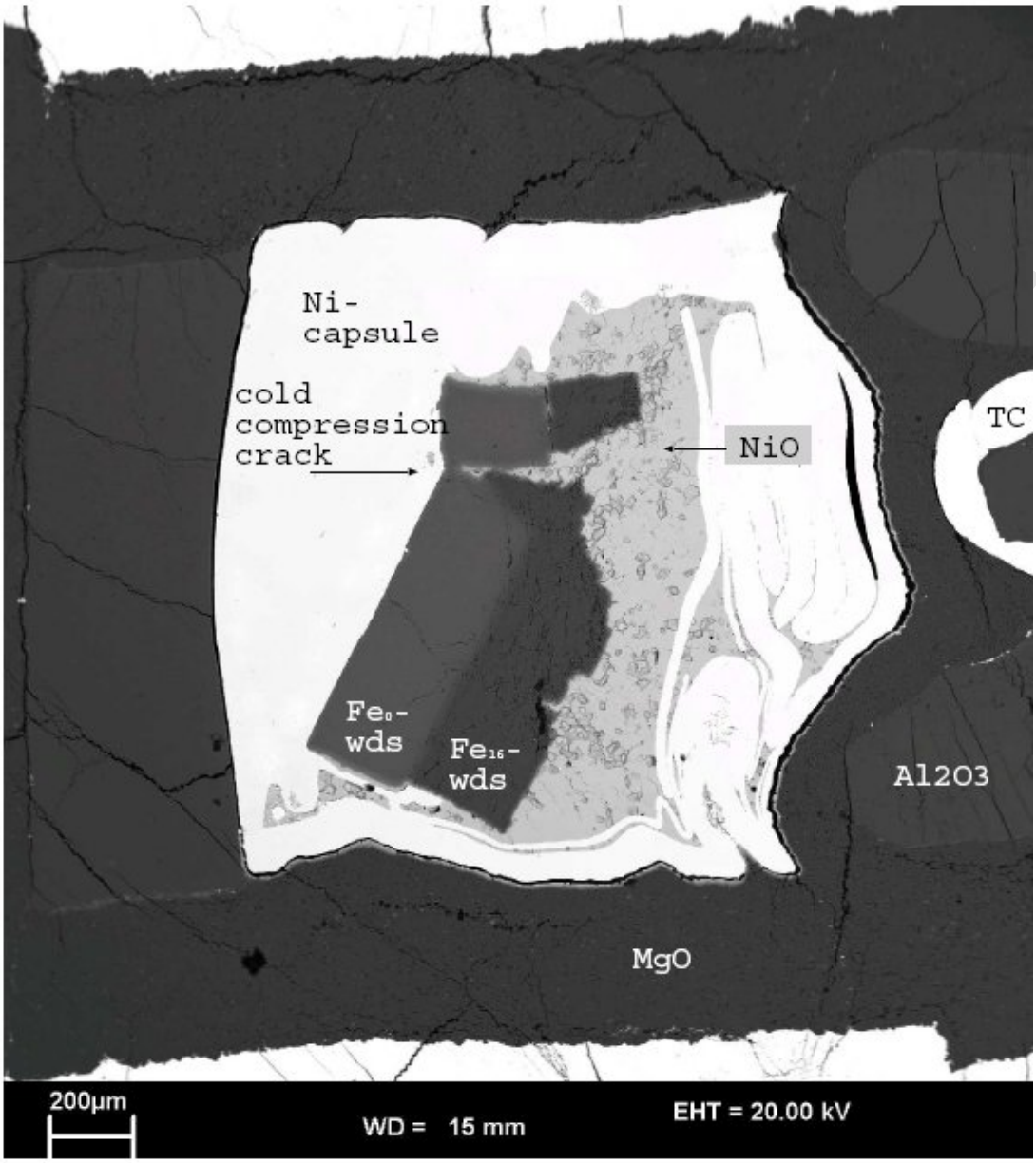

533
534
535 Fig. 1

536
537
538

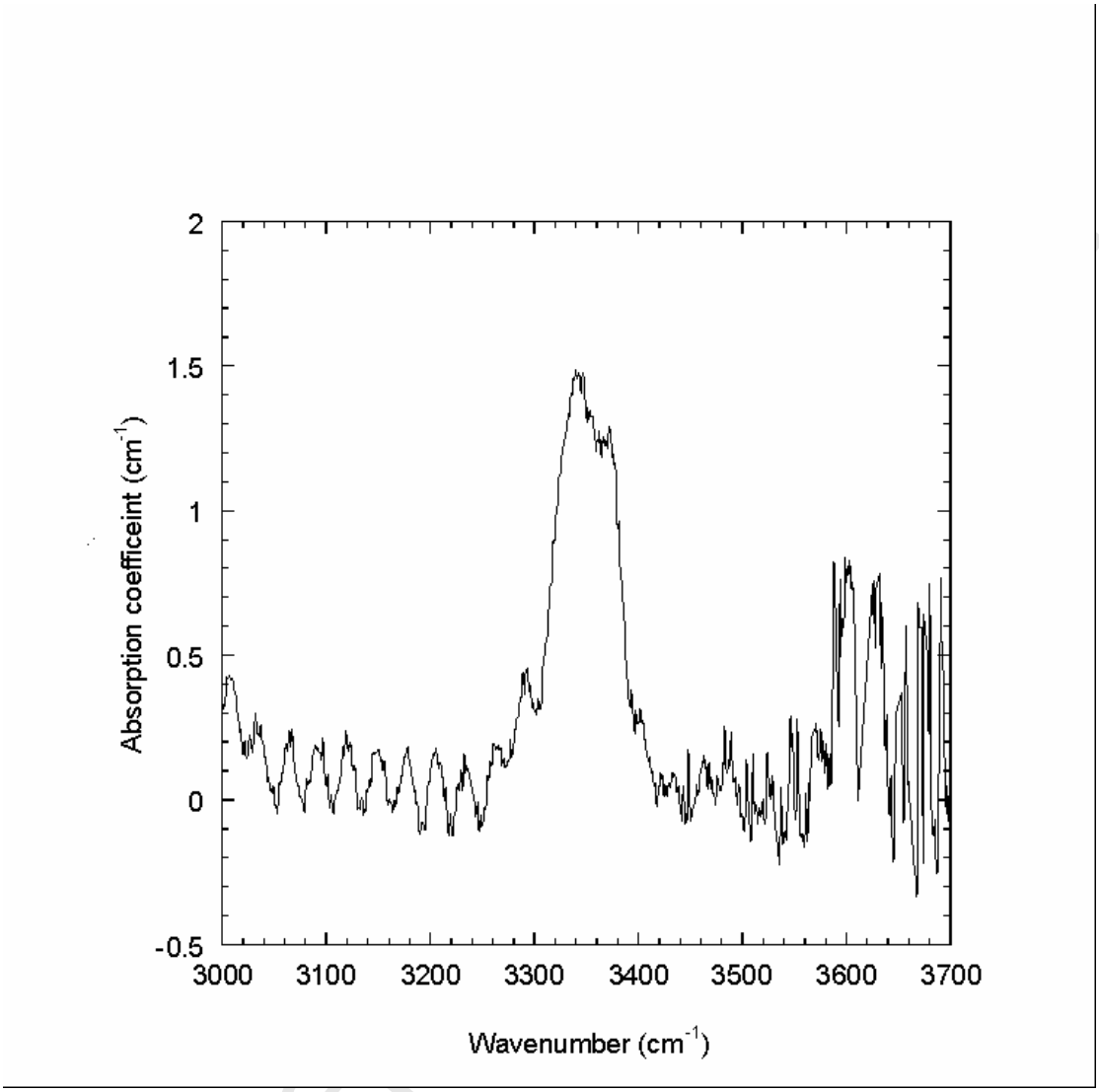

539
540
541 Fig. 2

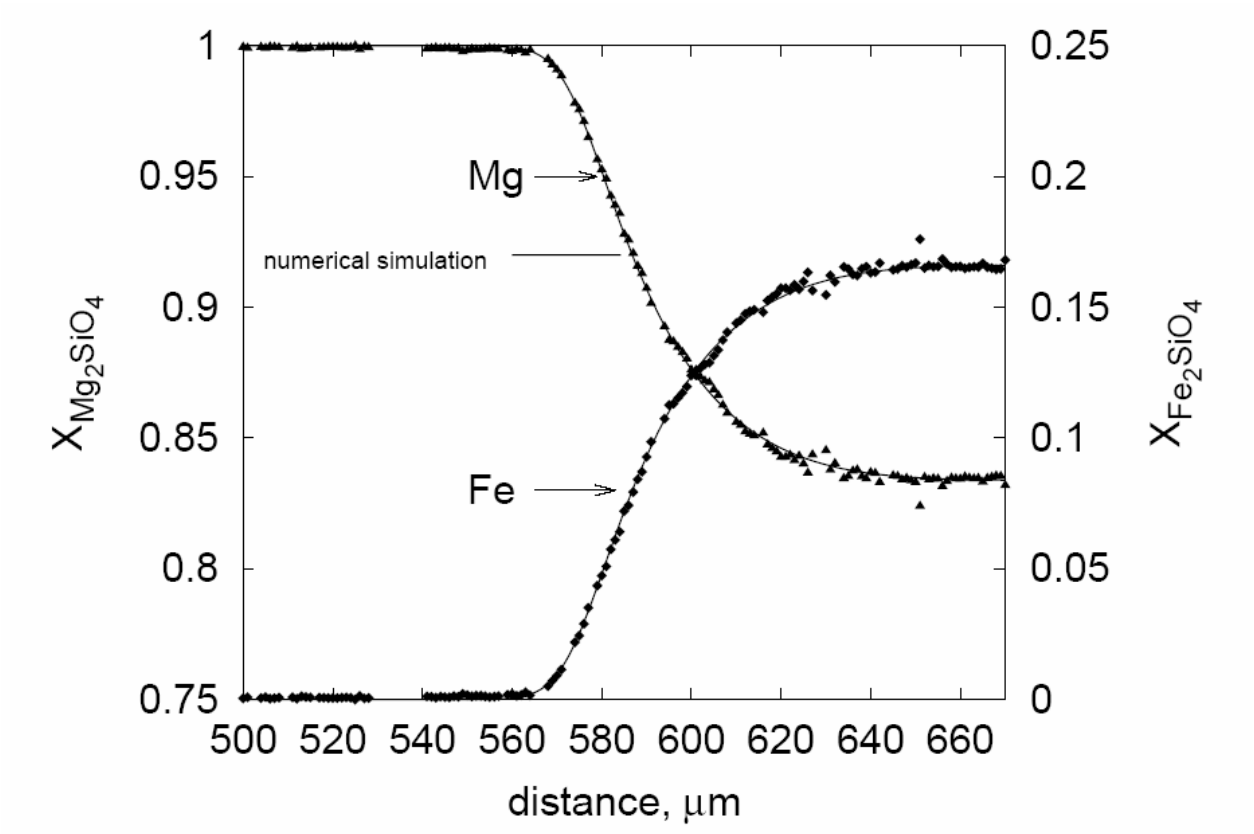

Fig. 3a

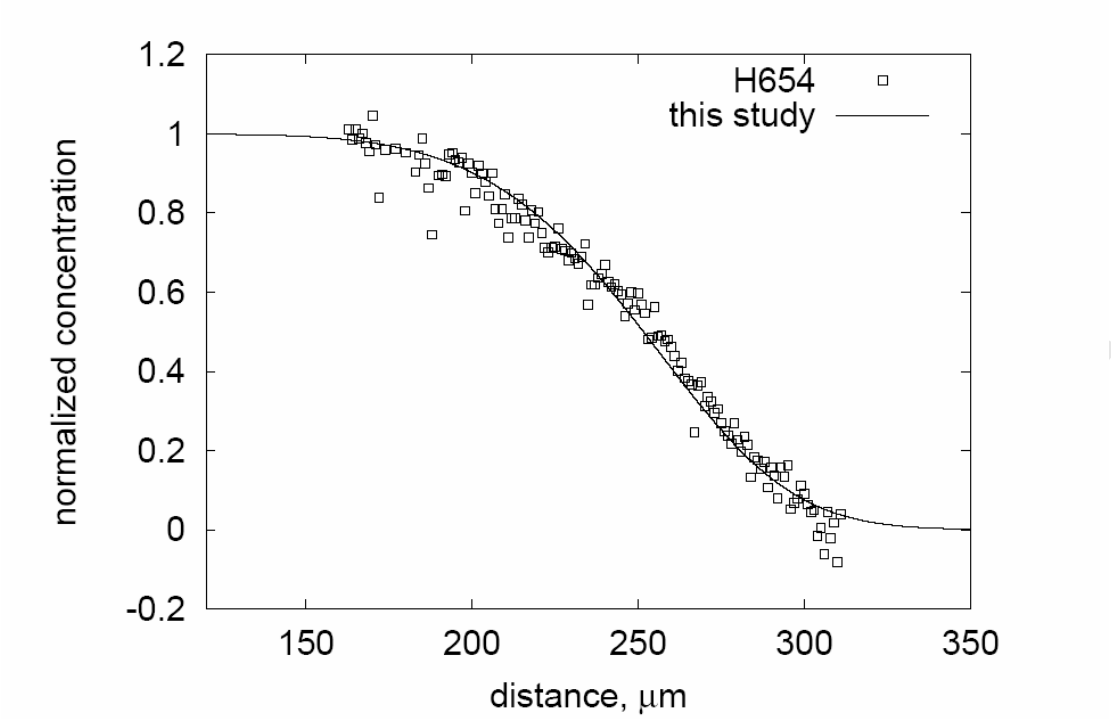

Fig. 3b

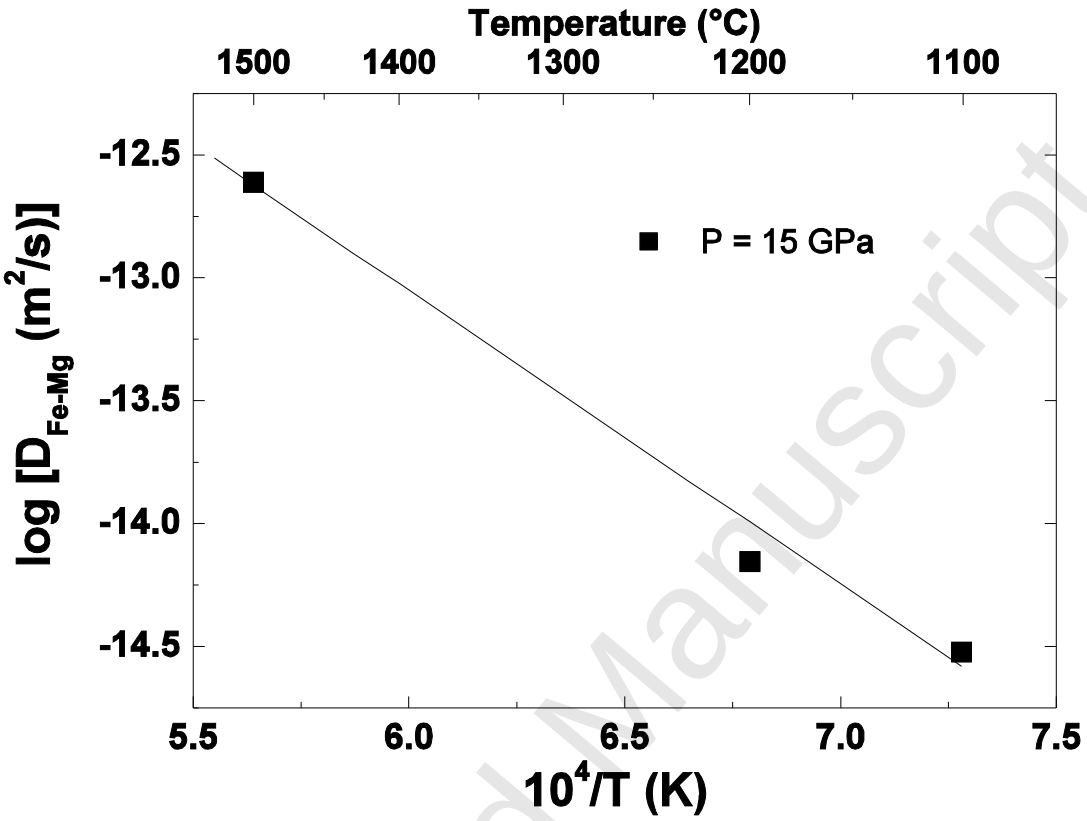

Fig. 4a

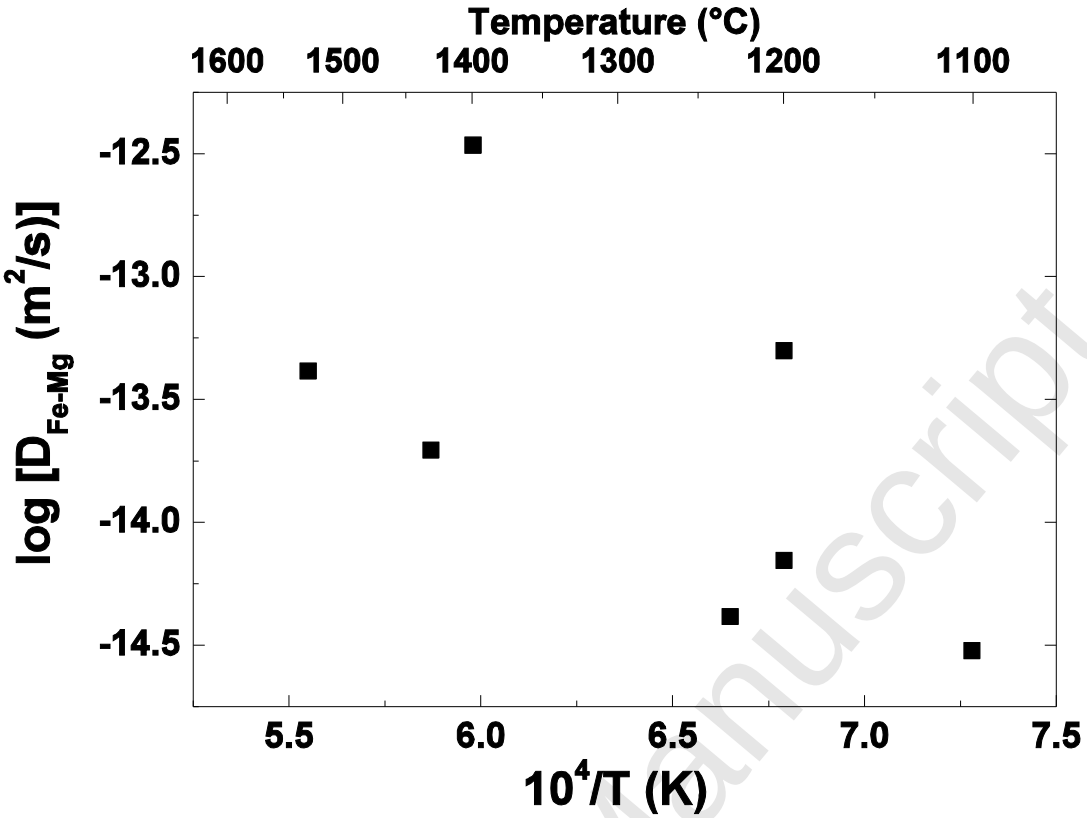

Fig. 4b

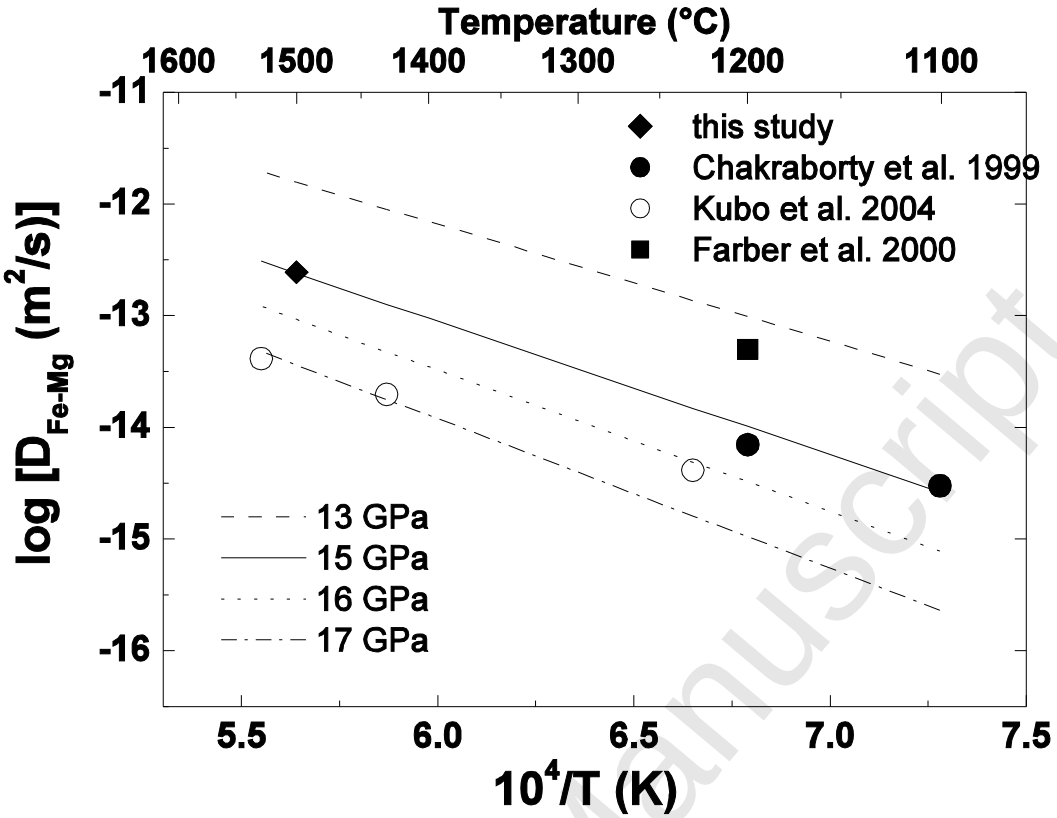

Fig. 4c